

Probing quantum chaos through singular-value correlations in sparse non-Hermitian SYK model

Pratik Nandy ^{1,2,*} Tanay Pathak ^{1,†} and Masaki Tezuka ^{3,‡}

¹*Center for Gravitational Physics and Quantum Information, Yukawa Institute for Theoretical Physics, Kyoto University, Kitashirakawa Oiwakecho, Sakyo-ku, Kyoto 606-8502, Japan*

²*RIKEN Interdisciplinary Theoretical and Mathematical Sciences Program (iTHEMS), Wako, Saitama 351-0198, Japan*

³*Department of Physics, Kyoto University, Kitashirakawa Oiwakecho, Sakyo-ku, Kyoto 606-8502, Japan*

Exploring the spectral properties of non-Hermitian systems presents a substantial theoretical challenge due to the presence of a complex eigenvalue spectrum. Singular values for such systems are inherently real and non-negative, and the techniques used for Hermitian systems can be used with ease. As a prototypical example of such systems, we investigate the singular-value spectrum of a non-Hermitian extension of the sparse Sachdev-Ye-Kitaev (SYK) model, a solvable toy model of quantum chaos and quantum gravity with significant interest in digital quantum simulation. Our findings reveal a congruence between the statistics of singular values and those of the analogous Hermitian Gaussian ensembles. An increase in sparsity results in the model deviating from its chaotic behavior, a phenomenon precisely captured by both short and long-range correlations in the singular-value spectrum. These findings indicate the existence of a critical sparsity threshold, beyond which the chaotic nature of the model breaks down, suggesting a potential collapse of holographic duality in such systems.

Introduction: Spectral statistics serve as a critical tool for probing the energy levels in quantum systems, offering insights into the dynamics within quantum chaos and Random Matrix Theory (RMT) [1–8]. Short-range level statistics such as the ratio of consecutive level spacings [9] and the long-range correlations such as the Spectral Form Factor (SFF) [10–15] reveal the symmetries and randomness in the system. The latter has also been understood from the semiclassical gravity [16] and measured in many-body scenarios [17, 18]. Analogously, the upsurge in research has been directed towards unraveling the quantum chaotic properties of open quantum systems [19–21] described by non-Hermitian Hamiltonians [22–26]. This connotes a departure from conventional methods suited for Hermitian systems and necessitates new methods for spectral analysis [27–33]. One such method approaches through the Singular Value Decomposition (SVD) [34], which facilitates a straightforward generalization of the frameworks used for Hermitian systems with real and non-negative singular values. Consequently, this enables us to define the singular spacing ratios [34] and singular form factor (σ FF) [35] in a much more elegant manner capturing transitions from integrability to chaos, many-body localization [35, 36], and the non-Hermitian skin effect [37–39]. Outside this domain, SVD has also found applications in generalizing entanglement entropy for non-Hermitian transition matrices in AdS/CFT correspondence [40].

In this paper, we utilize the SVD framework to study the quantum chaotic properties and their transitions in the sparse, non-Hermitian version of the Sachdev-Ye-Kitaev (SYK) model [41, 42]. Standing as a quintessential archetype for quantum chaos and possessing a dual gravitational theory at low temperatures [43], the SYK

model (see See [44, 45] for comprehensive reviews) can be adapted into sparse variants [46–50], maintaining its chaotic nature up to a critical sparsity threshold [51, 52]. This adaptation holds theoretical considerations in holography as well as the practical significance for the deployment of the SYK model on quantum processors [53, 54], where managing a sparse matrix is more viable. Our focus is particularly drawn to the influence that sparsity exerts on the average singular value spacing ratio, denoted by $\langle r_\sigma \rangle$, and the σ FF, which serves as an extension of the conventional $\langle r \rangle$ -value [9] and the SFF in Hermitian systems, respectively. Additionally, we introduce *singular complexity*, inspired by spectral complexity, a boundary dual to the volume of the Einstein-Rosen bridge in gravitational theories [55]. Our findings suggest that these metrics proficiently encapsulate the transition from chaos to integrability in the non-Hermitian SYK model, as we outline in the following sections.

Non-Hermitian sparse SYK model: The prototypical model we consider is the 4-body non-Hermitian sparse SYK model (nSYK) [41, 42], given by the following Hamiltonian

$$H_{\text{nSYK}}^{\text{sparse}} = \sum_{1 \leq a < b < c < d \leq N} x_{abcd} (J_{abcd} + iM_{abcd}) \psi_a \psi_b \psi_c \psi_d. \quad (1)$$

where J_{abcd} and M_{abcd} are the independent random couplings drawn from the Gaussian ensemble with zero mean and variance $\langle J_{abcd}^2 \rangle = \langle M_{abcd}^2 \rangle = 6/(pN^3)$ (see [56, 57] for clean SYK model), and p is the sparsity parameter. The couplings M_{abcd} explicitly break the Hermiticity of the Hamiltonian [46, 51]. The variables ψ_k are the Majorana fermions obeying Clifford algebra $\{\psi_a, \psi_b\} = \delta_{ab}$. Additionally, the random variables $x_{ijkl} \in \{0, 1\}$ intro-

duce an element of sparsity p to the Hamiltonian. The parameter p governs the probability of x_{abcd} being unity, thus determining the sparsity level within the Hamiltonian. A fully *dense* model is characterized by $x_{abcd} = 1$ or $p = 1$ for all combinations of $\{a, b, c, d\}$, aligning with the original nSYK Hamiltonian [58–61]. Conversely, a completely sparse model would have $x_{abcd} = 0$ or $p = 0$ for all combinations, representing the other extreme [46]. The addition of sparsity effectively reduces the total number of independent terms in the Hamiltonian from $O(N^4)$ to $O(pN^4) \sim O(kN)$, where k is defined in (4). Yet, the probabilistic nature of x_{abcd} implies that the exact number of non-zero terms in $H_{\text{nSYK}}^{\text{sparse}}$ is not fixed but rather determined by the probability p . We follow [52] without fixing the total number of terms in the sparse Hamiltonian in each realization.

Singular value decomposition and singular value statistics: In Hermitian systems, the eigenspectrum of the Hamiltonian is a key indicator of chaotic dynamics. The eigenvalues E_n are real, allowing for the definition of consecutive level spacings $s_n = E_{n+1} - E_n$, as an ordered list. For large Hilbert spaces, the average consecutive level spacing ratio r_n is defined as $r_n = \min(s_n, s_{n+1})/\max(s_n, s_{n+1})$ with $\langle r \rangle = \text{mean}(r_n)$ being the *average r value* [9]. Its usefulness lies in simplifying the numerical analysis by bypassing the need to unfold the spectrum for level statistics. While $\langle r \rangle$ -value is well-defined for Hermitian systems, it falls short in applying for non-Hermitian systems where eigenvalues are complex, and thus an ordered sequence of level spacings is not feasible. In such scenarios, one may consider complex spacing ratios [27] and correspondingly the statistics of complex eigenvalues. However, an alternate proposal suggests focusing on singular values derived from the singular value decomposition (SVD) of the Hamiltonian [34]. SVD is expressed as $H = U\Sigma V^\dagger$, where U and V are unitary matrices, and Σ is a diagonal matrix containing the real and non-negative singular values σ_i [62]. In Hermitian matrices, singular values are simply the absolute values of the eigenvalues, whereas, in non-Hermitian matrices, their relationship is more complex [63].

The singular values of a non-Hermitian matrix H can be computed by the *Hermitization* process [64], which involves constructing a new matrix \mathbb{H} , twice the dimension of H . This larger matrix incorporates both H and its Hermitian conjugate H^\dagger in a block structure [64]

$$\mathbb{H} = \begin{pmatrix} \mathbb{0} & H \\ H^\dagger & \mathbb{0} \end{pmatrix} \Rightarrow \mathbb{H}^2 = \begin{pmatrix} HH^\dagger & \mathbb{0} \\ \mathbb{0} & H^\dagger H \end{pmatrix}. \quad (2)$$

The eigenvalues of \mathbb{H} are $\{\pm\sigma_n\}$, precisely containing the singular values of H . This is equivalent to constructing an effective Hamiltonian $H_{\text{eff}} = \sqrt{H^\dagger H}$ or $H_{\text{eff}} = \sqrt{HH^\dagger}$ so that the eigenvalues of H_{eff} represent the singular values of H [64]. Such construction of a Hermitized matrix resembles the formulation of the Wishart SYK model and

System	$N = 20$	$N = 22$	$N = 24$	$N = 26$	$N = 28$	$N = 30$
$\langle r \rangle_{\text{RMT}}$	0.6744	0.5996	0.5307	0.5996	0.6744	0.5996
$\langle r_\sigma \rangle_{\text{nSYK}}$	0.6744	0.5997	0.5307	0.5996	0.6745	0.5995

TABLE I. The $\langle r_\sigma \rangle$ -values for the non-Hermitian *dense* SYK model for different system sizes $N = 20$ (10000), $N = 22$ (6000), $N = 24$ (2000), $N = 26$ (1000), $N = 28$ (100), and $N = 30$ (50), where the parenthesis includes the number of samples taken. Based on the $\langle r_\sigma \rangle$ values, we identify the periodicity as $N \bmod 8 = 0$ (GOE), 2, 6 (GUE), and 4 (GSE) [67]. These GOE, GUE, and GSE correspond to the eigenvalue statistics of the Hermitian matrices.

The values are in precise agreement (within numerical accuracy) with the $\langle r \rangle_{\text{RMT}}$ -values for large N results in [9].

its supersymmetric version, comprised of non-Hermitian conserved charges or supercharges [65, 66].

Given the singular values $\{\sigma_i\}$ of the corresponding non-Hermitian Hamiltonian H , one analogously defines $\lambda_n = \sigma_{n+1} - \sigma_n$ as the *singular value spacings*. Consequently, the *singular-value-spacing ratio* $r_{\sigma,n}$ is defined analogous to the r -ratio as [34]

$$r_{\sigma,n} = \frac{\min(\lambda_n, \lambda_{n+1})}{\max(\lambda_n, \lambda_{n+1})}, \quad \langle r_\sigma \rangle = \text{mean}(r_{\sigma,n}). \quad (3)$$

Referred to as the $\langle r_\sigma \rangle$ -value, they adhere to statistical distributions akin to those observed for non-Hermitian Hamiltonians, similar to the $\langle r \rangle$ -value distributions for Hermitian matrices. This framework has been instrumental in addressing the 38-fold symmetry classification in non-Hermitian systems [34].

Table I showcases the $\langle r_\sigma \rangle$ -value for the *dense* non-Hermitian SYK model for varying system sizes N , representing the total number of fermions. The data is juxtaposed with corresponding eigenvalue statistics of Hermitian Gaussian ensembles, revealing a striking correlation emphasizing the utility of the $\langle r_\sigma \rangle$ -value in non-Hermitian systems. Similar to its Hermitian counterpart, we observe an $N \bmod 8$ periodicity using singular value statistics: $N \bmod 8 = 0$ corresponds to GOE, $N \bmod 8 = 2$ and 6 corresponds to GUE, and $N \bmod 8 = 4$ corresponds to GSE for the eigenvalue statistics of the Hermitian matrices. Figure 1 correspondingly shows the consecutive *singular level-spacing distribution* $p_\sigma(\lambda)$ for $N = 24$ (GOE), $N = 26$ (GUE) and $N = 28$ (GSE) respectively, which are *approximated* by the analogous Hermitian Wigner-Dyson distribution [1]. Note that we are comparing the singular value statistics of non-Hermitian matrices to the eigenvalue statistics of Hermitian matrices. The singular value correlations in Hermitian matrices are generally weaker than the eigenvalue correlations and exhibit different spacing ratios [34]. However, the nSYK falls into the different non-Hermitian symmetry classes, which can also be used to show the validity of the singular value statistics [59].

SVD in sparse non-Hermitian SYK model: We now turn our attention to the sparse variant of the model,

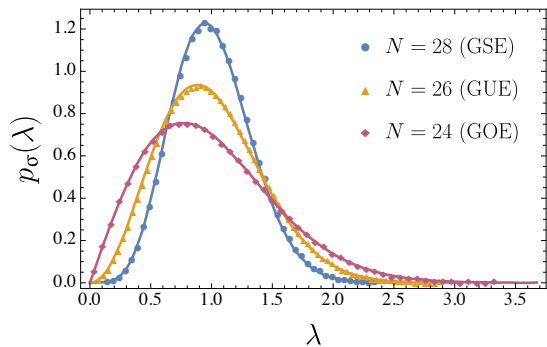


FIG. 1. The consecutive singular level-spacing distribution in the non-Hermitian dense SYK model for $N = 24$ (2000) (GOE), 26 (1000) (GUE), and 28 (100) (GSE) with the corresponding realizations shown in the brackets. The solid lines represent distribution for GOE, GUE, and GSE respectively taking matrices of size $10^4 \times 10^4$ with averaging over 1000 realizations.

which is governed by the sparsity parameter p . Figure 2 illustrates the dependence of p on $\langle r_\sigma \rangle$ -value for different system sizes. Each system size, representing a distinct ensemble, is depicted in a unique color. The dotted lines mark the expected values for Poisson statistics and the Hermitian ensemble, as specified in Table I. It is observed that the Hamiltonian (1) retains its chaotic nature up to a critical level of sparsity denoted by p_{crit} . This chaotic behavior is also corroborated by the $\langle r_\sigma \rangle$ -ratio presented in Table I. Consequently, we define a transition point p_{crit} beyond which the Hamiltonian (1) ceases to exhibit chaotic dynamics. Such transition point is obtained by considering approximately 99% of the corresponding $\langle r_\sigma \rangle$ value at $p = 1$ [52]. Notably, as the system size increases, this transition point migrates towards lower sparsity levels. When the sparsity is sufficiently low, the $\langle r_\sigma \rangle$ -value aligns with the Poisson limit, signifying the Hamiltonian's transition to complete integrability. Note that when a term of the Hamiltonian very weakly breaks a degeneracy, the resulting spectrum has r_σ values close to zero, which can cause the $\langle r_\sigma \rangle$ value to fall below the Poisson limit.

In conjunction with the above, the relationship between the critical sparsity p_{crit} and the system size N is also noteworthy. The critical value diminishes as the system size increases. This reduction follows a power-law trend, best described by fitting the data to the curve [52]

$$p_{\text{crit}} = kN \binom{N}{4}^{-1} \approx \frac{24k}{N^3}, \quad (4)$$

in the large N limit. where the decrease is proportional to $1/N^3$ and the constant k is approximately 1.68, as determined by the fitting process. This scaling behavior is consistent with that observed for the sparse Hermitian SYK model, as reported in [51, 52].

Spectral and Singular form factor: Contrary to the

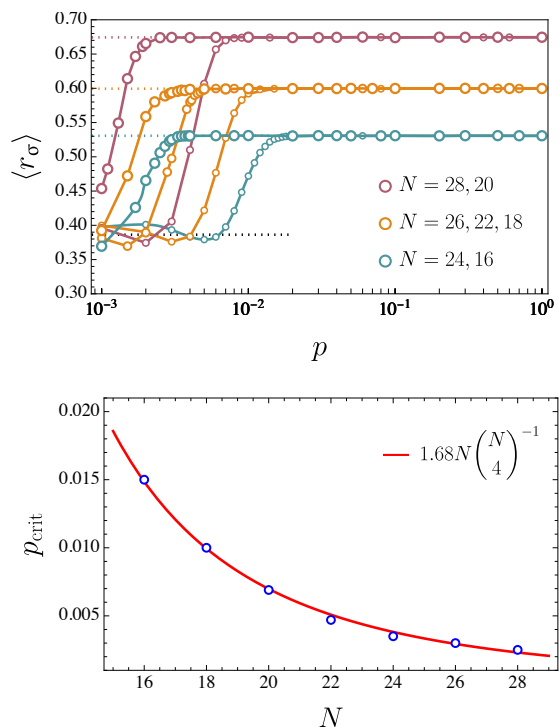


FIG. 2. (Top) Variation of $\langle r_\sigma \rangle$ -value with various level of sparsity p . The size of the circle varies with N i.e., the largest N corresponds to the leftmost plot for each color. At low sparsity, the $\langle r_\sigma \rangle$ matches with the corresponding random matrix ensemble until a threshold p_{crit} is reached, after which $\langle r_\sigma \rangle$ drops to the Poissonian value, indicating a hint of integrability. The estimated errors for the values obtained are smaller than the markers in the plot. (Bottom) The finite-size dependence of the threshold or the critical value p_{crit} . It decreases as the system size increases. The decrease scales as $1/N^3$ with large system size, as given in (4).

singular value statistics, the SFF probes the long-range eigenvalue correlations. It is defined as the Fourier transform of two-point eigenvalue correlation pairs [12–14]. For systems exhibiting quantum chaos, the SFF displays a characteristic dip-ramp-plateau pattern. The initial dip, evident in the early-time regime, is a non-universal trait influenced by the detailed nature of the energy spectrum [10]. This dip extends until a timescale known as the *Thouless time* (t_{Th}) [68, 69] or *ramp time* [15] beyond which the energy difference surpasses the inverse of t_{Th} , referred to as the *Thouless energy* [70]. Subsequently, a ramp emerges at t_{Th} , indicative of eigenvalue repulsion, a phenomenon that mirrors the SFF behavior predicted by RMT [14, 15] and underscores the chaotic dynamics of the Hamiltonian. Moreover, this ramp hints at the presence of a holographic dual to the corresponding theory. Beyond the *Heisenberg time* [71, 72], which scales inversely to the mean level spacing, the SFF reaches a plateau that depends on the system size. In contrast, integrable systems typically bypass the ramp stage and

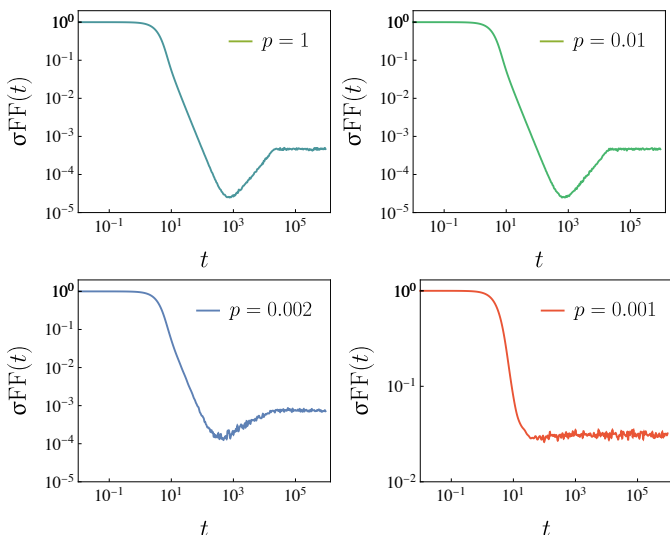


FIG. 3. Behavior of $\sigma\text{FF}(t)$ for various sparsity parameter p . The linear ramp ceases to exist as the sparsity increases. The system parameters are $N = 26$ (GUE) with 1000 Hamiltonian realizations. Here we choose the Gaussian filter with $\alpha = 3.27$, which lies within the prescribed range in [52].

saturate directly from the dip to the plateau regime. SFF in sparse SYK models has been thoroughly investigated in recent literature [47, 48, 51, 52]. Several other generalizations for SFF in non-Hermitian and open systems have also been proposed [31–33].

Analogous to the SFF, the singular form factor (σFF) is defined as [35]

$$\sigma\text{FF}(t) = \frac{1}{L^2} \langle |Z_\sigma(it)|^2 \rangle = \frac{1}{L^2} \left\langle \left| \sum_n e^{-i\sigma_n t} \right|^2 \right\rangle, \quad (5)$$

where $Z_\sigma(it) = \sum_n e^{-i\sigma_n t}$ is the infinite-temperature partition function of singular values, which can be further expressed as the overlap between the time-evolved right or left singular vectors governed by the effective Hamiltonian $\sqrt{H^\dagger H}$ or $\sqrt{H H^\dagger}$ respectively [35]. Here the angle brackets indicate an ensemble average, which is particularly relevant in the context of a disordered system since σFF is not self-averaging [72].

Figure 3 shows the distinct dip-ramp-plateau pattern exhibited by σFF for the Hamiltonian (1), across varying degrees of sparsity. In this work, we consider a system size of $N = 26$ and analyze the outcomes from 1000 independent realizations of the Hamiltonian to ensure robust statistical analysis. To reduce the oscillations in the dip region, we use the filter function $Y_\sigma(\alpha, t)$ [68] such that

$$\sigma\text{FF}(t) = \left\langle \frac{|Y_\sigma(\alpha, t)|^2}{|Y_\sigma(\alpha, 0)|^2} \right\rangle, \quad (6)$$

Here the Gaussian filter function for the singular values is defined as $|Y_\sigma(\alpha, t)|^2 = \left| \sum_n e^{-\alpha \sigma_n^2} e^{-i\sigma_n t} \right|^2$. Similar

to the eigenspectrum [68, 69], it ensures that the dominant contribution is received from the bulk of the singular value spectrum. Here α is an N -dependent parameter that controls the Gaussianity of the spectrum. This filtering is performed for the usual spectrum, without unfolding it. For the latter case, an equivalent of *connected unfolded* SFF [69, 73] can be defined. We employ the filter function on the singular values by choosing $\alpha = 3.27$, which lies inside the range given in [52] for $N = 26$. Filter functions for SFF have also recently been shown to be associated with quantum channels [74].

A notable observation in Fig. 3 is a parallelism between the behavior of σFF in non-Hermitian systems and the SFF in Hermitian systems. This similarity underscores the efficacy of σFF as a robust indicator for quantum chaos in non-Hermitian frameworks. In regimes of lower sparsity, the presence of the ramp is evident, signifying the retention of chaotic dynamics within this parameter space. It remains pronounced until a critical sparsity threshold is reached. Beyond this juncture, the linear ramp—a signature trait of non-integrable systems—ceases to manifest, indicating a shift towards integrability and a departure from chaotic behavior.

Figure 4 shows the variation of Thouless time (t_{Th}), for $N = 26$, with sparseness parameter p . The t_{Th} is calculated by considering the time at which the σFF of the system considered first intersects the SFF of the GUE random matrices [15]. To determine the intersection point precisely, we consider the fractional error function $\epsilon(t) := \left| \frac{\sigma\text{FF}(t) - \sigma_{\text{ramp}}(t)}{\sigma_{\text{ramp}}(t)} \right|$ [68] indicating the deviation of the computed σFF to the linear-fitted function for the ramp $\sigma_{\text{ramp}}(t)$ for $p = 1$. We consider the value t as the Thouless time or ramp time t_{Th} , where the fractional error $\epsilon(t)$ reaches 20%. The red line shows the fitting $t_{\text{Th}} \approx a/p^b + c$ with $a = 1.923$, $b = 0.8767$ and $c = 0.007$. Curiously, this fitting follows closely to the $1/p$ scaling in contrast to the $1/p^2$ scaling in Hermitian systems [52]. Such distinction is possible since the singular values and the eigenvalues are inherently different (see the Supplemental Material [75] S1). Yet, we do not rule out the possibility of the scaling of the exponent b with N .

Spectral complexity for singular values - Singular complexity: Within the framework of the AdS/CFT correspondence [76, 77], a particular spectral measure has been proposed to capture the essence of long-range spectral correlations. This measure, known as *spectral complexity*, is proposed to be a dual quantity of the Einstein-Rosen bridge [55] in the gravitational theory, serving as an analog for the computational and circuit complexity [78]. In a similar spirit, we define *singular complexity* at infinite temperature as

$$C_\sigma(t) = \frac{1}{L^2} \sum_{\sigma_i \neq \sigma_j} \left[\frac{\sin(t(\sigma_i - \sigma_j)/2)}{(\sigma_i - \sigma_j)/2} \right]^2, \quad (7)$$

designed to be suitable for non-Hermitian systems. At

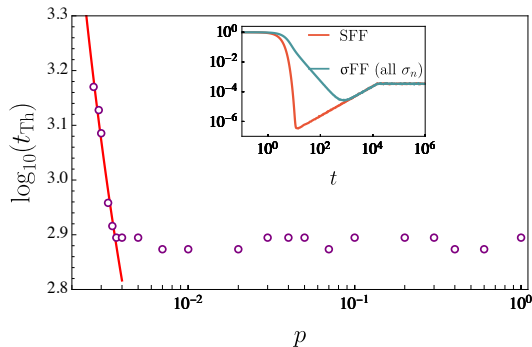


FIG. 4. (Main plot) Thouless time (ramp time) with respect to sparsity parameter. The red line is the fit $t_{\text{Th}} \approx a/p^b + c$ with $a = 1.923$, $b = 0.8767$ and $c = 0.007$. (Inset) The behavior of SFF and the σFF for the Hermitian dense SYK₄ model. The system parameters are $N = 26$ with 1000 random Hamiltonian realizations taken. The σFF (green line) is computed considering all the positive singular values. It reduces to the SFF after taking the appropriate rescaling of the singular vectors and singular values, which otherwise equals the eigenvalues (with appropriate signs).

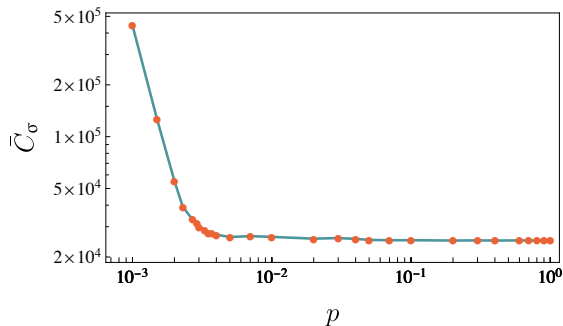


FIG. 5. Behavior of the saturation of the singular complexity with different sparseness for $N = 26$ with 1000 random Hamiltonian realizations.

early times, it grows quadratically, followed by a linear growth and plateau regime (see Supplemental Material [75] S2 for more details). The early time behavior mirrors the behavior of spread complexity [79, 80] based on the Krylov space approach [81]. The plateau value can be obtained analytically by taking the long-time average

$$\bar{C}_\sigma = \lim_{t_f \rightarrow \infty} \frac{1}{t_f} \int_0^{t_f} C_\sigma(t) dt = \frac{2}{L^2} \sum_{\sigma_i \neq \sigma_j} \frac{1}{(\sigma_i - \sigma_j)^2}, \quad (8)$$

which only depends on the difference between the singular values. In the Hermitian case, such saturation values have been studied for quantum billiards [82] and mixed-field Ising model [83], capturing the *spectral rigidity*. Integrable systems saturate at higher values compared to chaotic ones due to the presence of level repulsion, as evident from the equivalent eigenspectrum of (8).

Figure 5 depicts the saturation of singular complexity at varying levels of sparsity, which maintains a magnitude

order of $O(10^4)$ until it encounters a critical threshold. Beyond this threshold, there is a marked escalation at lower sparsity levels signaling a level-repulsion between the singular values. This critical value is dependent on the system size N , and for $N = 26$, it occurs within the sparsity regime $0.003 \lesssim p_{\text{crit}} \lesssim 0.004$. This value resembles the expected $\langle r_\sigma \rangle$ -value shown in Fig. 2.

Exhibiting chaotic dynamics is considered to be a crucial constraint that possesses a holographic dual geometry. While this discussion does not explore the specifics of such geometry, some proposals exist in the literature [58, 84–86]. The breakdown of chaotic nature suggests that such dual geometry corresponding to a non-Hermitian system may be compromised at low sparsity.

Conclusion and Outlook: Drawing on the foundational work [34] on the applicability of SVD in non-Hermitian systems, our study addresses the quantum chaotic attributes of the sparse SYK model across varying levels of sparsity. The complex eigenvalues inherent to non-Hermitian Hamiltonians pose challenges to the generalization of traditional eigenvalue statistics. This complexity persists despite strides made with complex spacing ratios [27] and the DSFF [28, 29]. Nonetheless, recent advancements propose a novel perspective by focusing on singular values as opposed to eigenvalues within the non-Hermitian framework. Unlike their complex counterparts, singular values are inherently real and non-negative, aligning with the real eigenvalues in Hermitian systems upon appropriate alignment with singular vectors, as detailed in the Supplemental Material [75] S1.

Our investigation underscores that the statistical analysis of singular values, which elucidates short-range correlations, coupled with the σFF and singular complexity, illuminating long-range correlations among singular values, serve as potent indicators of the chaos within non-Hermitian systems. As such, exploring the holographic bulk dual of singular complexity may offer insights into a potential holographic counterpart for non-Hermitian systems, especially the effective range of k in (4) in relation to $2d$ de Sitter (dS₂) gravity [84], which we leave for future work. Moreover, these tools adeptly reflect the shift towards integrability as sparsity intensifies. Such transition differs from other chaotic-integrable transitions by two-point interactions observed in the SYK model [87]. We envision that these features will be exhibited in other correlation measures such as higher spacing ratios [88–90] and the number variance [31, 68, 91, 92].

Parallel research avenues have explored the efficacy of sparse Hamiltonians [46, 47] within quantum processors [53, 54], maintaining chaotic dynamics to a substantial degree of sparsity. Notably, the SYK model retains its holographic duality even at minimal sparsity levels [51, 52]. Our study contributes to the burgeoning field of non-Hermitian systems in the realm of open-system dynamics, proposing a framework for the extrapolation of quantum chaotic properties within these systems. This might serve

as the benchmark results for the simulation of sparse non-Hermitian systems on quantum processors.

Acknowledgements: We would like to thank Hugo A. Camargo, Adolfo del Campo, Aurélie Chenu, Antonio M. García-García, Luca V. Iliesiu, Yiyang Jia, Hosho Katsura, and Tadashi Takayanagi for fruitful discussions, comments, and suggestions on the draft. Numerical computations were performed in the *Sushiki* workstation using the computational facilities of YITP. P.N. thanks the Berkeley Center for Theoretical Physics (BCTP), University of California for hosting him through the Adopting Sustainable Partnerships for Innovative Research Ecosystem (ASPIRE) program of Japan Science and Technology Agency (JST), Grant No. JPMJAP2318 during the final stages of the work. This work is supported by the Japan Society for the Promotion of Science (JSPS) Grants-in-Aid for Transformative Research Areas (A) “Extreme Universe” No. JP21H05190 (P.N.) and JP21H05182, JP21H05185 (M.T.). The Yukawa Research Fellowship of T.P. is supported by the Yukawa Memorial Foundation and JST CREST (Grant No. JPMJCR19T2). The work of M.T. was partially supported by the JSPS Grants-in-Aid for Scientific Research (KAKENHI) Grants No. JP20K03787 and JST CREST (Grant No. JPMJCR24I2).

Authors’ names are listed in alphabetical order.

* pratik@yukawa.kyoto-u.ac.jp

† pathak.tanay@yukawa.kyoto-u.ac.jp

‡ tezuka@scphys.kyoto-u.ac.jp

- [1] M.L. Mehta, *Random Matrices* (Academic Press, 1991).
- [2] O. Bohigas, M. J. Giannoni, and C. Schmit, “Characterization of chaotic quantum spectra and universality of level fluctuation laws,” *Phys. Rev. Lett.* **52**, 1–4 (1984).
- [3] Eugene P. Wigner, “Characteristic Vectors of Bordered Matrices With Infinite Dimensions,” *Annals of Mathematics* **62**, 548–564 (1955).
- [4] Eugene P. Wigner, “Characteristics Vectors of Bordered Matrices with Infinite Dimensions II,” *Annals of Mathematics* **65**, 203–207 (1957).
- [5] Freeman J. Dyson, “Statistical Theory of the Energy Levels of Complex Systems. I,” *Journal of Mathematical Physics* **3**, 140–156 (1962).
- [6] Freeman J. Dyson, “Statistical Theory of the Energy Levels of Complex Systems. II,” *Journal of Mathematical Physics* **3**, 157–165 (1962).
- [7] Michael Victor Berry, M. Tabor, and John Michael Ziman, “Level clustering in the regular spectrum,” *Proceedings of the Royal Society of London. A. Mathematical and Physical Sciences* **356**, 375–394 (1977).
- [8] M. V. Berry and M. Tabor, “Closed orbits and the regular bound spectrum,” *Proceedings of the Royal Society of London. Series A, Mathematical and Physical Sciences* **349**, 101–123 (1976).
- [9] Y. Y. Atas, E. Bogomolny, O. Giraud, and G. Roux, “Distribution of the ratio of consecutive level spacings in random matrix ensembles,” *Phys. Rev. Lett.* **110**, 084101 (2013).
- [10] Oded Agam, Boris L. Altshuler, and Anton V. Andreev, “Spectral statistics: From disordered to chaotic systems,” *Phys. Rev. Lett.* **75**, 4389–4392 (1995).
- [11] Thomas Guhr, Axel Muller-Groeling, and Hans A. Weidenmuller, “Random matrix theories in quantum physics: Common concepts,” *Phys. Rept.* **299**, 189–425 (1998).
- [12] Luc Leviandier, Maurice Lombardi, Rémi Jost, and Jean Paul Pique, “Fourier transform: A tool to measure statistical level properties in very complex spectra,” *Phys. Rev. Lett.* **56**, 2449–2452 (1986).
- [13] Joshua Wilkie and Paul Brumer, “Time-dependent manifestations of quantum chaos,” *Phys. Rev. Lett.* **67**, 1185–1188 (1991).
- [14] E. Brézin and S. Hikami, “Spectral form factor in a random matrix theory,” *Phys. Rev. E* **55**, 4067–4083 (1997).
- [15] Jordan S. Cotler, Guy Gur-Ari, Masanori Hanada, Joseph Polchinski, Phil Saad, Stephen H. Shenker, Douglas Stanford, Alexandre Streicher, and Masaki Tezuka, “Black Holes and Random Matrices,” *JHEP* **05**, 118 (2017), [Erratum: *JHEP* 09, 002 (2018)].
- [16] Phil Saad, Stephen H. Shenker, and Douglas Stanford, “A semiclassical ramp in SYK and in gravity,” (2018), [arXiv:1806.06840 \[hep-th\]](https://arxiv.org/abs/1806.06840).
- [17] Adway Kumar Das *et al.*, “Proposal for many-body quantum chaos detection,” (2024), [arXiv:2401.01401 \[cond-mat.stat-mech\]](https://arxiv.org/abs/2401.01401).
- [18] Hang Dong *et al.*, “Measuring Spectral Form Factor in Many-Body Chaotic and Localized Phases of Quantum Processors,” (2024), [arXiv:2403.16935 \[quant-ph\]](https://arxiv.org/abs/2403.16935).
- [19] Sergey Denisov, Tetyana Laptjeva, Wojciech Tarnowski, Dariusz Chruściński, and Karol Życzkowski, “Universal spectra of random Lindblad operators,” *Phys. Rev. Lett.* **123**, 140403 (2019).
- [20] Yifeng Yang, Zhenyu Xu, and Adolfo del Campo, “Decoherence rate in random Lindblad dynamics,” *Phys. Rev. Res.* **6**, 023229 (2024).
- [21] Pratik Nandy, Apollonas S. Matsoukas-Roubeas, Pablo Martínez-Azcona, Anatoly Dymarsky, and Adolfo del Campo, “Quantum Dynamics in Krylov Space: Methods and Applications,” (2024), [arXiv:2405.09628 \[quant-ph\]](https://arxiv.org/abs/2405.09628).
- [22] Carl M. Bender and Stefan Boettcher, “Real spectra in nonHermitian Hamiltonians having PT symmetry,” *Phys. Rev. Lett.* **80**, 5243–5246 (1998).
- [23] Naoyuki Shibata and Hosho Katsura, “Dissipative spin chain as a non-Hermitian Kitaev ladder,” *Phys. Rev. B* **99**, 174303 (2019).
- [24] Yuto Ashida, Zongping Gong, and Masahito Ueda, “Non-Hermitian physics,” *Adv. Phys.* **69**, 249–435 (2021).
- [25] Julien Cornelius, Zhenyu Xu, Avadh Saxena, Aurelia Chenu, and Adolfo del Campo, “Spectral Filtering Induced by Non-Hermitian Evolution with Balanced Gain and Loss: Enhancing Quantum Chaos,” *Phys. Rev. Lett.* **128**, 190402 (2022).
- [26] Apollonas S. Matsoukas-Roubeas, Federico Roccati, Julien Cornelius, Zhenyu Xu, Aurelia Chenu, and Adolfo del Campo, “Non-Hermitian Hamiltonian deformations in quantum mechanics,” *JHEP* **01**, 060 (2023).
- [27] Lucas Sá, Pedro Ribeiro, and Tomaž Prosen, “Complex spacing ratios: A signature of dissipative quantum chaos,” *Phys. Rev. X* **10**, 021019 (2020).

- [28] Jiachen Li, Tomaz Prosen, and Amos Chan, “Spectral Statistics of Non-Hermitian Matrices and Dissipative Quantum Chaos,” *Phys. Rev. Lett.* **127**, 170602 (2021).
- [29] Jiachen Li, Stephen Yan, Tomaz Prosen, and Amos Chan, “Spectral form factor in chaotic, localized, and integrable open quantum many-body systems,” (2024), [arXiv:2405.01641](https://arxiv.org/abs/2405.01641) [cond-mat.stat-mech].
- [30] Giorgio Cipolloni and Nicolo Grometto, “The Dissipative Spectral Form Factor for I.I.D. Matrices,” *J. Statist. Phys.* **191**, 21 (2024).
- [31] Antonio M. García-García, Lucas Sá, and Jacobus J. M. Verbaarschot, “Universality and its limits in non-Hermitian many-body quantum chaos using the Sachdev-Ye-Kitaev model,” *Phys. Rev. D* **107**, 066007 (2023).
- [32] Zhenyu Xu, Aurelia Chenu, Tomaz Prosen, and Adolfo del Campo, “Thermofield dynamics: Quantum Chaos versus Decoherence,” *Phys. Rev. B* **103**, 064309 (2021).
- [33] Yi-Neng Zhou, Tian-Gang Zhou, and Pengfei Zhang, “General properties of the spectral form factor in open quantum systems,” *Front. Phys. (Beijing)* **19**, 31202 (2024).
- [34] Kohei Kawabata, Zhenyu Xiao, Tomi Ohtsuki, and Ryuichi Shindou, “Singular-Value Statistics of Non-Hermitian Random Matrices and Open Quantum Systems,” *PRX Quantum* **4**, 040312 (2023).
- [35] Federico Roccati, Federico Balducci, Ruth Shir, and Aurélie Chenu, “Diagnosing non-Hermitian many-body localization and quantum chaos via singular value decomposition,” *Phys. Rev. B* **109**, L140201 (2024).
- [36] Ryusuke Hamazaki, Kohei Kawabata, and Masahito Ueda, “Non-hermitian many-body localization,” *Phys. Rev. Lett.* **123**, 090603 (2019).
- [37] V. M. Martínez Alvarez, J. E. Barrios Vargas, and L. E. F. Foa Torres, “Non-hermitian robust edge states in one dimension: Anomalous localization and eigenspace condensation at exceptional points,” *Phys. Rev. B* **97**, 121401(R) (2018).
- [38] Shunyu Yao and Zhong Wang, “Edge states and topological invariants of non-hermitian systems,” *Phys. Rev. Lett.* **121**, 086803 (2018).
- [39] Shu Hamanaka and Kohei Kawabata, “Multifractality of Many-Body Non-Hermitian Skin Effect,” (2024), [arXiv:2401.08304](https://arxiv.org/abs/2401.08304) [cond-mat.str-el].
- [40] Arthur J. Parzygnat, Tadashi Takayanagi, Yusuke Taki, and Zixia Wei, “SVD entanglement entropy,” *JHEP* **12**, 123 (2023).
- [41] Subir Sachdev and Jinwu Ye, “Gapless spin-fluid ground state in a random quantum heisenberg magnet,” *Phys. Rev. Lett.* **70**, 3339–3342 (1993).
- [42] A. Kitaev, “A simple model of quantum holography (part 1) and (part 2),” <https://online.kitp.ucsb.edu/online/joint98/kitaev/>, <https://online.kitp.ucsb.edu/online/entangled15/kitaev2/> (2015), talk given at KITP.
- [43] Juan Maldacena and Douglas Stanford, “Remarks on the Sachdev-Ye-Kitaev model,” *Phys. Rev. D* **94**, 106002 (2016).
- [44] Debanjan Chowdhury, Antoine Georges, Olivier Parcollet, and Subir Sachdev, “Sachdev-Ye-Kitaev models and beyond: Window into non-Fermi liquids,” *Rev. Mod. Phys.* **94**, 035004 (2022).
- [45] Vladimir Rosenhaus, “An introduction to the SYK model,” *J. Phys. A* **52**, 323001 (2019).
- [46] Shenglong Xu, Leonard Susskind, Yuan Su, and Brian Swingle, “A Sparse Model of Quantum Holography,” (2020), [arXiv:2008.02303](https://arxiv.org/abs/2008.02303) [cond-mat.str-el].
- [47] Masaki Tezuka, Onur Oktay, Enrico Rinaldi, Masanori Hanada, and Franco Nori, “Binary-coupling sparse Sachdev-Ye-Kitaev model: An improved model of quantum chaos and holography,” *Phys. Rev. B* **107**, L081103 (2023).
- [48] Takanori Anegawa, Norihiro Iizuka, Arkaprava Mukherjee, Sunil Kumar Sake, and Sandip P. Trivedi, “Sparse random matrices and Gaussian ensembles with varying randomness,” *JHEP* **11**, 234 (2023).
- [49] Elena Caceres, Anderson Misobuchi, and Rafael Pimentel, “Sparse SYK and traversable wormholes,” *JHEP* **11**, 015 (2021).
- [50] Elena Cáceres, Tyler Guglielmo, Brian Kent, and Anderson Misobuchi, “Out-of-time-order correlators and Lyapunov exponents in sparse SYK,” *JHEP* **11**, 088 (2023).
- [51] Antonio M. García-García, Yiyang Jia, Dario Rosa, and Jacobus J. M. Verbaarschot, “Sparse Sachdev-Ye-Kitaev model, quantum chaos and gravity duals,” *Phys. Rev. D* **103**, 106002 (2021).
- [52] Patrick Orman, Hrant Gharibyan, and John Preskill, “Quantum chaos in the sparse SYK model,” (2024), [arXiv:2403.13884](https://arxiv.org/abs/2403.13884) [hep-th].
- [53] Daniel Jafferis, Alexander Zlokapa, Joseph D. Lykken, David K. Kolchmeyer, Samantha I. Davis, Nikolai Lauk, Hartmut Neven, and Maria Spiropulu, “Traversable wormhole dynamics on a quantum processor,” *Nature* **612**, 51–55 (2022).
- [54] Bryce Kobrin, Thomas Schuster, and Norman Y. Yao, “Comment on ‘Traversable wormhole dynamics on a quantum processor’,” (2023), [arXiv:2302.07897](https://arxiv.org/abs/2302.07897) [quant-ph].
- [55] Luca V. Iliesiu, Márk Mezei, and Gábor Sárosi, “The volume of the black hole interior at late times,” *JHEP* **07**, 073 (2022).
- [56] Pak Hang Chris Lau, Chen-Te Ma, Jeff Murugan, and Masaki Tezuka, “Correlated disorder in the SYK₂ model,” *J. Phys. A* **54**, 095401 (2021).
- [57] Soshun Ozaki and Hosho Katsura, “Disorder-free Sachdev-Ye-Kitaev models: Integrability and a precursor of chaos,” *Phys. Rev. Res.* **7**, 013092 (2025).
- [58] Antonio M. García-García and Victor Godet, “Euclidean wormhole in the Sachdev-Ye-Kitaev model,” *Phys. Rev. D* **103**, 046014 (2021).
- [59] Antonio M. García-García, Lucas Sá, and Jacobus J. M. Verbaarschot, “Symmetry Classification and Universality in Non-Hermitian Many-Body Quantum Chaos by the Sachdev-Ye-Kitaev Model,” *Phys. Rev. X* **12**, 021040 (2022).
- [60] Antonio M. García-García, Yiyang Jia, Dario Rosa, and Jacobus J. M. Verbaarschot, “Replica symmetry breaking in random non-Hermitian systems,” *Phys. Rev. D* **105**, 126027 (2022).
- [61] Giorgio Cipolloni and Jonah Kudler-Flam, “Entanglement Entropy of Non-Hermitian Eigenstates and the Ginibre Ensemble,” *Phys. Rev. Lett.* **130**, 010401 (2023).
- [62] Michael A. Nielsen and Isaac L. Chuang, *Quantum Computation and Quantum Information: 10th Anniversary Edition* (Cambridge University Press, 2010).
- [63] Matthias Allard and Mario Kieburg, “Correlation functions between singular values and eigenvalues,” (2024), [arXiv:2403.19157](https://arxiv.org/abs/2403.19157) [math.PR].
- [64] Joshua Feinberg and A. Zee, “Non-hermitian random ma-

- trix theory: Method of hermitian reduction,” *Nuclear Physics B* **504**, 579–608 (1997).
- [65] Tianlin Li, Junyu Liu, Yuan Xin, and Yehao Zhou, “Supersymmetric SYK model and random matrix theory,” *JHEP* **06**, 111 (2017).
- [66] Lucas Sá and Antonio M. García-García, “Q-Laguerre spectral density and quantum chaos in the Wishart-Sachdev-Ye-Kitaev model,” *Phys. Rev. D* **105**, 026005 (2022).
- [67] Yi-Zhuang You, Andreas W. W. Ludwig, and Cenke Xu, “Sachdev-Ye-Kitaev Model and Thermalization on the Boundary of Many-Body Localized Fermionic Symmetry Protected Topological States,” *Phys. Rev. B* **95**, 115150 (2017).
- [68] Hrant Gharibyan, Masanori Hanada, Stephen H. Shenker, and Masaki Tezuka, “Onset of Random Matrix Behavior in Scrambling Systems,” *JHEP* **07**, 124 (2018), [Erratum: *JHEP* 02, 197 (2019)].
- [69] Tomoki Nosaka, Dario Rosa, and Junggi Yoon, “The Thouless time for mass-deformed SYK,” *JHEP* **09**, 041 (2018).
- [70] D. J. Thouless, “Maximum metallic resistance in thin wires,” *Phys. Rev. Lett.* **39**, 1167–1169 (1977).
- [71] László Erdős and Antti Knowles, “The Altshuler–Shklovskii Formulas for Random Band Matrices I: the Unimodular Case,” *Communications in Mathematical Physics* **333**, 1365–1416 (2015).
- [72] R. E. Prange, “The spectral form factor is not self-averaging,” *Phys. Rev. Lett.* **78**, 2280–2283 (1997).
- [73] Antonio M. García-García, Yiyang Jia, and Jacobus J. M. Verbaarschot, “Universality and Thouless energy in the supersymmetric Sachdev-Ye-Kitaev Model,” *Phys. Rev. D* **97**, 106003 (2018).
- [74] Apollonas S. Matsoukas-Roubeas, Mathieu Beau, Lea F. Santos, and Adolfo del Campo, “Unitarity breaking in self-averaging spectral form factors,” *Phys. Rev. A* **108**, 062201 (2023).
- [75] See Supplemental Materials with additional references [93, 94] at URL-will-be-inserted-by-publisher for detailed information on the comparison between singular values and eigenvalues and the behavior of the singular complexity.
- [76] Juan Martin Maldacena, “The Large N limit of superconformal field theories and supergravity,” *Adv. Theor. Math. Phys.* **2**, 231–252 (1998).
- [77] Edward Witten, “Anti-de Sitter space and holography,” *Adv. Theor. Math. Phys.* **2**, 253–291 (1998).
- [78] Ro Jefferson and Robert C. Myers, “Circuit complexity in quantum field theory,” *JHEP* **10**, 107 (2017).
- [79] Vijay Balasubramanian, Pawel Caputa, Javier M. Magan, and Qingyue Wu, “Quantum chaos and the complexity of spread of states,” *Phys. Rev. D* **106**, 046007 (2022).
- [80] Johanna Erdmenger, Shao-Kai Jian, and Zhuo-Yu Xian, “Universal chaotic dynamics from Krylov space,” *JHEP* **08**, 176 (2023).
- [81] Daniel E. Parker, Xiangyu Cao, Alexander Avdoshkin, Thomas Scaffidi, and Ehud Altman, “A Universal Operator Growth Hypothesis,” *Phys. Rev. X* **9**, 041017 (2019).
- [82] Hugo A. Camargo, Viktor Jahnke, Hyun-Sik Jeong, Keun-Young Kim, and Mitsuhiro Nishida, “Spectral and Krylov complexity in billiard systems,” *Phys. Rev. D* **109**, 046017 (2024).
- [83] Hugo A. Camargo, Kyoung-Bum Huh, Viktor Jahnke, Hyun-Sik Jeong, Keun-Young Kim, and Mitsuhiro Nishida, “Spread and spectral complexity in quantum spin chains: from integrability to chaos,” *JHEP* **08**, 241 (2024).
- [84] Antonio M. García-García, Lucas Sá, Jacobus J. M. Verbaarschot, and Jie Ping Zheng, “Keldysh wormholes and anomalous relaxation in the dissipative Sachdev-Ye-Kitaev model,” *Phys. Rev. D* **107**, 106006 (2023).
- [85] Wenhe Cai, Sizheng Cao, Xian-Hui Ge, Masataka Matsumoto, and Sang-Jin Sin, “Non-Hermitian quantum system generated from two coupled Sachdev-Ye-Kitaev models,” *Phys. Rev. D* **106**, 106010 (2022).
- [86] Sizheng Cao and Xian-Hui Ge, “Excitation transmission through a non-Hermitian traversable wormhole,” *Phys. Rev. D* **110**, 046022 (2024).
- [87] Antonio M. García-García, Bruno Loureiro, Aurelio Romero-Bermúdez, and Masaki Tezuka, “Chaotic-Integrable Transition in the Sachdev-Ye-Kitaev Model,” *Phys. Rev. Lett.* **120**, 241603 (2018).
- [88] Shashi C L Srivastava, Arul Lakshminarayanan, Steven Tomsovic, and Arnd Bäcker, “Ordered level spacing probability densities,” *Journal of Physics A: Mathematical and Theoretical* **52**, 025101 (2018).
- [89] S. Harshini Tekur, Udaysinh T. Bhosale, and M. S. Santhanam, “Higher-order spacing ratios in random matrix theory and complex quantum systems,” *Phys. Rev. B* **98**, 104305 (2018).
- [90] Ruth Shir, Pablo Martinez-Azcona, and Aurélia Chenu, “Full range spectral correlations and their spectral form factors in chaotic and integrable models,” (2023), [arXiv:2311.09292 \[quant-ph\]](https://arxiv.org/abs/2311.09292).
- [91] Ferdinand Evers and Alexander D. Mirlin, “Anderson transitions,” *Rev. Mod. Phys.* **80**, 1355–1417 (2008).
- [92] Antonio M. García-García and Jacobus J. M. Verbaarschot, “Spectral and thermodynamic properties of the Sachdev-Ye-Kitaev model,” *Phys. Rev. D* **94**, 126010 (2016).
- [93] Olivier Giraud, Nicolas Macé, Éric Vernier, and Fabien Alet, “Probing Symmetries of Quantum Many-Body Systems through Gap Ratio Statistics,” *Phys. Rev. X* **12**, 011006 (2022).
- [94] Eiki Iyoda, Hoshio Katsura, and Takahiro Sagawa, “Effective dimension, level statistics, and integrability of Sachdev-Ye-Kitaev-like models,” *Phys. Rev. D* **98**, 086020 (2018).

Supplemental Materials:

Probing quantum chaos through singular-value correlations in sparse non-Hermitian SYK model

Pratik Nandy, Tanay Pathak, and Masaki Tezuka

S1. From σ FF to SFF: Reduction to Hermitian systems

In Hermitian systems, a key observation is that the singular values correspond to the absolute values of the eigenvalues. This distinction is crucial, as it implies that the SFF and σ FF, exhibit fundamentally different behaviors. This difference is illustrated in the inset of Fig. 4, which depicts the dynamics of SFF and σ FF for the dense Hermitian SYK₄ model. The model is derived by setting $x_{abcd} = 1$ and $M_{abcd} = 0$ for all $\{a, b, c, d\}$ in its non-Hermitian counterpart (Eq. (1)). Replacing σ_n by eigenvalues E_n in Eq. (6), we get the analogous definition of filtered SFF.

System	$\langle r_\sigma \rangle$	$\langle r \rangle$	$\langle r_+ \rangle$	$\langle r_- \rangle$	$\langle r \rangle$ (2 blocks)
nSYK ($N = 20$)	0.4119	0.6743	0.6744	0.6744	0.4117
nSYK ($N = 22$)	0.4220	0.5994	0.5998	0.5991	0.4220
nSYK ($N = 24$)	0.4238	0.5303	0.5303	0.5302	0.4234

TABLE II. The Table shows the comparison between the singular value $\langle r_\sigma \rangle$ -value and the $\langle r \rangle$ -values for the *dense* Hermitian SYK model for different system sizes $N = 20$ (GSE), $N = 22$ (GUE), $N = 24$ (GOE). We take 1000 Hamiltonian realizations for each case. The Hermitian model is obtained by setting $x_{abcd} = 1$ and $M_{abcd} = 0$ for all $\{a, b, c, d\}$ in the Hamiltonian (1). Here the $\langle r_+ \rangle$ -value includes the positive eigenvalues while $\langle r_- \rangle$ -value includes the negative eigenvalues only. They are to be matched with the $\langle r \rangle_{\text{RMT}}$ values in Table I and [9]. The $\langle r_\sigma \rangle$ -values are compared with the $\langle r \rangle$ -value of 2 blocks (marked in blue) [52]. Explanation is given in the text.

Notably, the singular values offer a *weaker* effect compared to the eigenvalues, considering the ramp. However, to reduce the SFF from σ FF, we consider the following prescription. From SVD, we obtain two sets of vectors, the left and right singular vectors. They are related by

$$H |u_n\rangle = \sigma_n |v_n\rangle, \quad H^\dagger |v_n\rangle = \sigma_n |u_n\rangle, \quad (9)$$

where $\{\sigma_n\}$ are the singular values. For Hermitian systems, the eigenvalues are real, and the left ($|u_n\rangle$) and the right ($|v_n\rangle$) singular vectors are related with a factor of ± 1 . If the left and right singular vectors are equal, i.e., $|u_n\rangle = |v_n\rangle$ for some n , then the corresponding singular value exactly equals the eigenvalue i.e., $\sigma_n = E_n$. However, if they differ by a negative sign i.e., $|u_n\rangle = -|v_n\rangle$ for some n , then the corresponding singular value and the eigenvalue differs by a negative sign i.e., $\sigma_n = -E_n$. It is thus straightforward to identify such vectors such that the singular values can be directly mapped with the eigenvalues, and correspondingly compute the σ FF. In this case, the σ FF exactly equals the SFF as shown by the red line in the inset of Fig. 4.

Intriguingly, the Hermitian system exhibits a unique characteristic in its $\langle r_\sigma \rangle$ -value. As depicted in Table II, there is a notable distinction when comparing the $\langle r_\sigma \rangle$ -value to the $\langle r \rangle$ -values within the identical Hermitian SYK₄ model. Additionally, the $\langle r_+ \rangle$ -value and $\langle r_- \rangle$ -value were computed separately, considering only the positive and negative eigenvalues of the Hamiltonian, respectively. These ratios align with the overall $\langle r \rangle$ -value, which is anticipated since it solely accounts for the spacing between consecutive eigenvalues. Nonetheless, these individual ratios as well as the overall $\langle r \rangle$ -value do not correspond to the $\langle r_\sigma \rangle$ -value, which is identified as the $\langle r \rangle$ -value for two separate blocks before symmetry resolution. This discrepancy arises because, in Hermitian systems, the singular values are determined by the absolute magnitudes of the eigenvalues, leading to the computation of the $\langle r_\sigma \rangle$ -value mirroring the $\langle r \rangle$ -value for bifurcated blocks [34, 52, 93]. We anticipate such bifurcation has a similar effect of having the presence of conserved charges [66, 94]. Curiously, this phenomenon is exclusive to Hermitian and anti-Hermitian (with $J_{abcd} = 0$, $M_{abcd} \neq 0$) systems and echoes the discrepancy between the σ FF and SFF as shown in the inset of Fig. 4.

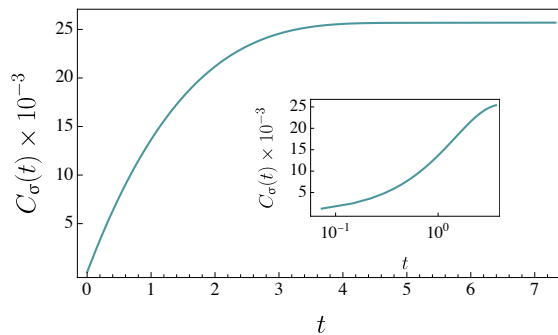


FIG. 6. Behaviour of the singular complexity with time for *dense* ($p = 1$) non-Hermitian SYK model. The system parameter is $N = 26$ with 1000 random Hamiltonian realizations taken. Inset shows the early time behavior of the complexity, which increases quadratically followed by linear growth and saturation.

S2. Behavior of singular complexity

Here we present the detailed behavior of singular complexity [55]. It is defined at finite temperature $T = 1/\beta$ as

$$C_{\sigma}(t) = \frac{1}{Z_{2\sigma}(\beta)L} \sum_{\sigma_i \neq \sigma_j} \left[\frac{\sin(t(\sigma_i - \sigma_j)/2)}{(\sigma_i - \sigma_j)/2} \right]^2 e^{-\beta(\sigma_i + \sigma_j)}. \quad (10)$$

Here $Z_{\sigma}(\beta) = \sum_n e^{-\beta\sigma_n}$ is the thermal *singular partition function*, constructed from the singular values of the corresponding non-Hermitian Hamiltonian. In the case of degeneracies, we keep the degenerate spectrum. The derivative of the singular complexity is related to the σ FF as

$$\frac{d^2}{dt^2} C_{\sigma}(t) = \frac{2}{L} \frac{Z_{\sigma}(\beta)^2}{Z_{\sigma}(2\beta)} \sigma\text{FF}(t) - \frac{2}{L}, \quad (11)$$

in a similar spirit to spectral complexity [55, 80] which can be checked. Focusing on the infinite temperature $\beta = 0$ limit, (10) takes a simpler form as in the main text:

$$C_{\sigma}(t) = \frac{1}{L^2} \sum_{\sigma_i \neq \sigma_j} \left[\frac{\sin(t(\sigma_i - \sigma_j)/2)}{(\sigma_i - \sigma_j)/2} \right]^2. \quad (7)$$

At early times, it grows quadratically as $C_{\sigma}(t) \approx (1 - 1/L)t^2$, followed by a linear growth and plateau regime. Figure 6 shows the time evolution of the infinite-temperature singular complexity (7) for the *dense* Hamiltonian for $N = 26$ and 1000 realizations. The complexity grows quadratically, followed by linear growth (inset) and saturation. The saturation value is elevated as the sparsity increases.